Oceland: A conceptual model for ocean-land-atmosphere interactions based on water balance equations

Luca Schmidt[a] , Cathy Hohenegger[a]

[a] *Max Planck Institute for Meteorology, Hamburg*

Corresponding author: Luca Schmidt, luca.schmidt@mpimet.mpg.de

ABSTRACT: The spatial distribution of precipitation is often misrepresented by General Circulation Models (GCM). In particular, precipitation tends to be underestimated over land and overestimated over ocean. One obstacle to resolving this longstanding issue is the lack of a general understanding of land-ocean-atmosphere interactions. More precisely, we do not have a fundamental theory that tells us which processes or physical quantities determine the partitioning of precipitation between land and ocean. In this study, we investigate whether large-scale constraints on this partitioning exist by using a conceptual box model based on water balance equations. With a small number of empirical but physically motivated parametrizations of the water balance components, we construct a set of coupled ordinary differential equations which describe the dynamical behaviour of the water vapour content of land and ocean atmospheres as well as the soil moisture content of land. We compute the equilibrium solution of this land-ocean-atmosphere system and analyze the sensitivity of the equilibrium state to model parameter choices. The results show that the ratio of mean land and ocean precipitation rates is primarily controlled by a scale-dependent atmospheric moisture transport parameter, the land fraction, and the permanent wilting point of the soil. We further demonstrate how the proposed model can be adapted for applications on both global and local scales to model, where the latter is useful to study e.g. island precipitation enhancement. For a global scale model configuration with one ocean and one land domain, we show that the precipitation ratio is constrained to a range between zero and one and are able to explain this behavior based on the underlying equations and the fundamental property of land to loose water through runoff.

1. Introduction

As human beings, we have a great interest in how Earth's climate and its change over time influence living conditions on the land surface. An important question in this respect is how much of the water that evaporates from the Earth's surface will precipitate over land as opposed to over the ocean. Unfortunately, even sophisticated General Circulation Models frequently fail to reproduce observed spatial patterns of precipitation, especially in the Tropics where precipitation amounts are high [Fiedler et al. (2020) and references therein]. However, more fundamentally, we are lacking a theoretical framework in which the partitioning of precipitation between land and ocean can be explained and analyzed with respect to its dependence on properties of the system which may or may not change over time. For instance, is the partitioning sensitive to land size? Do surface characteristics such as soil type matter or is it rather atmospheric conditions that dominate the behavior? It is the aim of this study to introduce a conceptual water balance model that reduces the complexity of the real world to a small number of physical processes that are key for understanding the precipitation partitioning. By investigating the sensitivity of the modelled precipitation partitioning to a variation of the model parameter values, this study can serve as a starting point for filling the gap of theoretical understanding described above.

Traditionally, hydrologists separate the Earth's hydrological cycle into an atmospheric branch, describing the sinks and sources of atmospheric moisture, and a terrestrial branch, describe the change of soil moisture [e.g.
Peixóto and Oort (1983)]. Evaporation and precipitation are the links that connect the two branches of the cycle. Since we aim at understanding the precipitation partitioning between land and ocean, it is convenient to choose a different perspective and think about an ocean and a land branch of the water cycle instead. The land and ocean branches are then linked through advective moisture transport between land and ocean atmospheres, and through runoff from the soil to the ocean.

The land branch in isolation has been studied intensively since the 1950s. In a pioneering land-atmosphere interaction study by Budyko and Drozdov (1953), the authors describe how an airstream that traverses a region imports atmospheric moisture at the windward contour, moistens or dries depending on the relative magnitude of mean precipitation and evaporation, and exports moisture at the leeward contour. In this one-dimensional framework known as the Budyko model, precipitation in the region can be expressed as a sum of two components: water that is advected from outside the region and water that previously evaporated from the surface inside the region. The relative contribution of the two components to total precipitation and, hence, the dependence of regional precipitation on advected moisture relative to local recycling through evapotranspiration, can be expressed as a water recycling coefficient. Important studies that used observations to estimate the water balance components and compute recycling coefficients include Brubaker et al. (1993), who formulated a two-dimensional Budyko model and investigated precipitation recycling in four innercontinental areas and Eltahir and Bras (1994), who focused on the Amazon region and refined the 2D model by allowing for a horizontally heterogeneous precipitation and evapotranspiration field (see Burde and Zangvil (2001) for a comprehensive review of the different adaptations of Budyko's framework and their limitations). A shortcoming of most recycling studies is the dependence of recycling coefficients on the size of the region of interest. The larger the region, the more precipitating water will be derived from within the region. Ent et al. (2010) circumvented this problem by taking a global perspective and defining recycled water as previously evaporated from any point on the land surface and advected water as evaporated from any point on the ocean surface. All mentioned studies show that precipitation recycling contributes significantly to land precipitation, especially in hotspot regions of land-atmosphere interactions such as the Sahel region, the Amazon or mountainous regions in Asia.

An alternative to estimating the water balance components from observations is to use analytical parametrizations. In water-limited areas, evapotranspiration is a function of soil moisture as described by e.g. Manabe (1969) or more recently updated in Seneviratne et al. (2010). Applied to the Budyko recycling framework, this turns the total precipitation into a function of soil moisture, mean advected precipitation, domain size and environmental parameters such as wind speed and potential evapotranspiration. The variability of the latter parameters introduces considerable randomness of precipitation in the real world and limits the utility of the Budyko model when being fixed to constant values. Rodriguez-Iturbe et al. (1991) and Entekhabi et al. (1992) address this issue by modulating mean parametric environmental conditions with Gaussian white noise. Both found that the system preferentially resides in a very dry or very moist soil moisture state for sufficiently high amplitudes of environmental variability. This finding suggests that even such a simple model offers an explanation for hydrological extremes such as droughts in continental regions.

What are the physical mechanisms that makes precipitation soil moisture-dependent? Broadly speaking, two lines of arguments were developed. The first one predicts a mostly positive feedback between precipitation and soil moisture, arguing that the enhanced latent heat flux over wet soils favors precipitating convection either through direct water input that can be recycled [e.g. Zangvil et al. (1993)] or by destabilizing the vertical profile in the air aloft [Schär et al. (1999), Findell and Eltahir (2003)]. Hohenegger et al. (2009) points out that the sign of this feedback mechanism can depend on model resolution and the choice of parametrization schemes. The second line of argument explains the soil moisture-precipitation feedback through mesoscale circulations that develop due to different Bowen ratios of wet and dry soil patches Segal and Arritt (1992). Such circulations may drive convective systems from rather moist to rather dry surface areas and contribute to a homogenization of soil moisture [Lynn et al. (1998), Hohenegger and Stevens (2018)]. However, Froidevaux et al. (2014) found that synoptic background winds can also displace convective air from drier soils, where convection was initiated, to wetter soils where the atmospheric conditions favor the onset of precipitation. Hence, the sign of the soil moisture feedback related to mesoscale processes is unclear.

The circulation argument has direct implications for our initial question about precipitation partitioning between land and ocean. In the context of Tropical islands, several studies showed that precipitation is enhanced over land due to sea breezes induced by daytime differential heating [Qian (2008), Cronin et al. (2015)]. Even though island precipitation enhancement is often associated with energy balance arguments which are not considered in this work, other factors such as island size [Sobel et al. (2011), Cronin et al. (2015), Wang and Sobel (2017), Ulrich and Bellon (2019)] and background wind speed [Sobel et al. (2011), Wang and Sobel (2017)] seem to matter, too, and these factors might be independent of the occurrence of sea breezes. We will return to the case of islands in the last part of this paper and explore what a purely water balance based approach can teach us about precipitation enhancement in such small-scale systems.

2. Model description

In this study, we want to understand the controlling factors for precipitation partitioning between land and ocean. Specifically, we ask whether fundamental constraints for this partitioning arise from water balance equations. To this end, we propose a box model as sketched in Figure 1 with

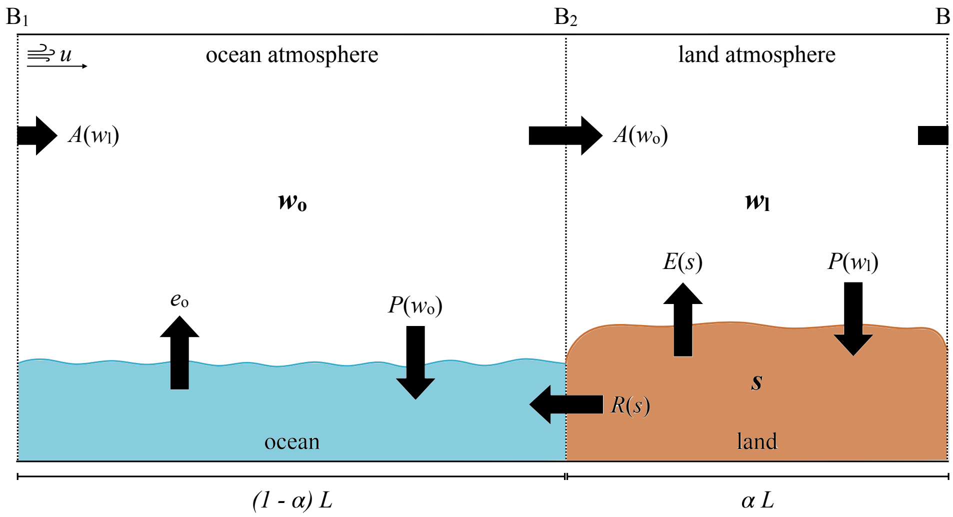

FIG. 1. Closed model sketch and water vapor pass distribution.

an ocean domain, denoted by subscript ‘o’, and a land domain, denoted by subscript ‘l’. The relative size of the two domains is given by the land fraction parameter α. Each of the two domains contains a ground box at the bottom (ocean or land) and an atmospheric box aloft. While the horizontal extent of the model is prescribed by length L, the downward/upward vertical extent of the ground/atmospheric boxes is taken to be infinite. The model has periodic boundary conditions, i.e. topologically, it resembles the wall of a cylinder with the right boundary of the land domain connecting to the left boundary of the ocean domain. This turns the model into a closed system in which water is conserved and which does not interact with any external environment. Such a *closed* model (CM) can be used to describe, for example, the entire globe or the full Tropics if net water exchange with the Extratropics can be assumed to be negligible. Later, in section 5, we introduce an *open* model (OM) formulation suitable for regional systems in which case boundary values are provided by synoptic-scale conditions and the modelled area can act as a net sink or source of moisture. In this case, water is still conserved in a global sense but not necessarily within the model.

a. Water balance equations

We further assume that the model boxes have well-mixed properties and that all water fluxes between them can be expressed as functions of their mean moisture content, i.e. the moisture state of the boxes. For atmospheric boxes, we use the mean water vapour pass w in mm, and for the land box the unitless mean relative soil moisture saturation s to describe the moisture state. As the ocean is considered fully saturated at all times, we don't need to assign a moisture variable to it. Hence, the full information on the moisture state of the land-ocean-atmosphere system at any given time t in days is given by the set of state variables $\{w_\mathrm{o}(t), w_\ell(t), s(t)\}$.

Following earlier studies by Peixóto and Oort (1983) and Brubaker et al. (1991), we describe the time-evolution of the state variables by coupled water balance equations in which moisture sinks and sources are represented by water fluxes between the boxes:

$$\frac{ds}{dt} = \frac{1}{nz_\mathrm{r}}\left[P(w_\ell) - R(s, w_\ell) - E(s)\right] \tag{1}$$

$$\frac{dw_\ell}{dt} = E_\ell(s) - P(w_\ell) + A_\ell(w_\ell, w_\mathrm{o}) \tag{2}$$

$$\frac{dw_\mathrm{o}}{dt} = E_\mathrm{o} - P(w_\mathrm{o}) + A_\mathrm{o}(w_\ell, w_\mathrm{o}). \tag{3}$$

Note, that the time-dependence of s, w_ℓ and w_o is implicit in Equations (1) to (3). The relevant fluxes, which are indicated by black arrows in Figure 1, are precipitation P from atmosphere to ground boxes, evapotranspiration E_ℓ from soil to land atmosphere, ocean evaporation E_o to the ocean atmosphere, runoff R from soil to ocean and advection A between the atmospheric boxes. All fluxes are given as spatial mean flux rates in mm/day ('mean' being frequently omitted in the remainder of this text). This is, in order to obtain the total moisture change in mm^2/day, Equations (1) and (2) would need to be multiplied by land domain size αL and Equation (3) by ocean domain size $(1-\alpha)L$. The advection terms A_ℓ and A_o refer to the *net* advection rate into the land and ocean atmosphere, respectively, and are positive for a net moisture import and negative for net moisture export. Note that the total net advection of a closed system vanishes, i.e. $\alpha A_\ell + (1-\alpha)A_\mathrm{o} = 0$. Dimensionless soil porosity n, hydrologically active soil depth z_r in mm and E_o are constant model parameters. An implicit assumption of this water balance approach is that the water holding capacity of the atmosphere does not change significantly over long enough timescales which we consider here.

b. Parametrizations

While the conservation of water is a fundamental condition, there are no simple fundamental laws governing the water fluxes between the model boxes. Instead, we need to turn to empirical relationships between the flux quantities and moisture state variables, as has been previously done by Rodriguez-Iturbe et al. (1991). We adopt the parametrization of runoff as the fraction R_{f} of precipitation that does not infiltrate the soil,

$$R(s, w_\ell) = R_{\mathrm{f}}(s) P(w_\ell), \tag{4}$$

with

$$R_{\mathrm{f}}(s) = \epsilon s^r, \tag{5}$$

and the two empirical dimensionless parameters $\epsilon \approx 1$ and $r \approx 2$. Equation (5) tells us that runoff intensifies as the soil moistens. It proves to be convenient to combine precipitation and runoff in Eqn. (1) to $P(w_\ell) - R(s, w_\ell) = P(w_\ell)\Phi(s)$, where we introduce the infiltration function $\Phi(s) = 1 - R_{\mathrm{f}} = 1 - \epsilon s^r$. Note that this parametrization assumes that runoff discharge happens uniformly across the land domain and that its water does not participate in any secondary processes that could moisten the soil.

For precipitation, Rodriguez-Iturbe et al. (1991) followed the approach of Budyko and Drozdov (1953) and obtain an expression for precipitation that is dependent on soil moisture which assumes that precipitation is a sum of an advected component and another component that originates from local evaporation from the surface. In this framework, the advected precipitation component is assumed to be known and is set to a fixed value. This is not a desirable construction in our case where precisely the interaction of land and ocean through advection is one main focus. Instead, we use the empirical parametrization of precipitation as a function mean water vapor pass, w, introduced by Bretherton et al. (2004). They find that the precipitation rate over tropical oceanic regions shows an exponential relationship with w,

$$P(w) = \exp\left[a\left(\frac{w}{w_{\mathrm{sat}}} - b\right)\right]. \tag{6}$$

Equation (6) introduces three parameters, two empirical dimensionless parameters $a \approx 15.6$ and $b \approx 0.6$ and the saturated water vapor pass $w_{\rm sat}$ in mm. Lacking a corresponding expression for extratropical ocean regions and land in general, we make the explicit assumption that Eqn. (6) holds everywhere and that the three parameters are the same over ocean and land. This assumption is rather crude and has major implications for the results presented in Section 4 as will be discussed in greater detail later on.

The qualitative dependence of evapotranspiration E_ℓ on soil moisture saturation is long-known, see e.g. Budyko (1956) or more recently and slightly modified in Seneviratne et al. (2010). E_ℓ is close to zero for soil moisture saturation values below the permanent wilting point, $s < s_{\rm pwp}$, increases approximately linearly in a transition range between the permanent wilting point and a critical value close to the field capacity, $s_{\rm pwp} < s < s_{\rm fc}$, and reaches a plateau for higher s-values, $s > s_{\rm fc}$, where evapotranspiration is nearly constant. The E_ℓ value of the plateau is denoted by potential evapotranspiration $E_{\rm p}$, an energy-dependent parameter that increases with increasing radiative energy input. In this work, $E_{\rm p}$ will be set to a constant value. For computational convenience, we parametrize evapotranspiration by the following smooth function which has the qualitative properties described above,

$$E_\ell(s) = \frac{E_{\rm p}}{2}\left[\tanh\left(10\left(s - \frac{s_{\rm pwp} + s_{\rm fc}}{2}\right)\right) + 1\right]. \tag{7}$$

Equation (7) implies that the entire land box is either covered by a single vegetation type or that a combination of vegetation types can be modelled by means of an effective mean value of $s_{\rm pwp}$, $s_{\rm fc}$ and $E_{\rm p}$. Unlike the land, the ocean is always fully saturated and its evaporation flux is energy-dependent in a similar way as $E_{\rm p}$. As we assume constant energetic conditions in this model, we treat the ocean evaporation rate as a constant model parameter with $E_{\rm o} \approx 3\,$mm/day.

It remains to find expressions for the *mean net* advection rates into the land and ocean atmospheres, hereafter just land/ocean advection rates. The net total advection flux into a given box is the difference between the moisture entering, $w_{\rm in}$, and leaving the box, $w_{\rm out}$, per unit time. This moisture transport is driven by a mean background wind velocity u in mm/day which we assume to be constant across the model domain. Total advection in mm^2/day can then be expressed as

$$A_{\rm tot} = (w_{\rm in} - w_{\rm out})u. \tag{8}$$

TABLE 1. Parameter ranges for closed model Monte Carlo simulations with uniform sampling.

Parameter	Minimum	Maximum	Range choice motivated by
s_{pwp}	0.2	0.54	Hagemann and Stacke (2015)
s_{fc}	0.5	0.84	Hagemann and Stacke (2015)
e_{p} [mm/day]	4.1	4.5	Rodriguez-Iturbe et al. (1991)
$nZ\mathrm{r}$ [mm]	90.0	110.0	Rodriguez-Iturbe et al. (1991)
e_{o} [mm/day]	2.8	3.2	C. Hohenegger, private communications
ϵ	0.9	1.1	Rodriguez-Iturbe et al. (1991)
r	2.0	2.0	fixed due to computational method, Rodriguez-Iturbe et al. (1991)
a	11.4	15.6	Bretherton et al. (2004)
b	0.522	0.603	Bretherton et al. (2004)
w_{sat} [mm]	65.0	80.0	Bretherton et al. (2004)
α	0.0	1.0	full possible range
u [m/s]	1.0	10.0	reasonable range for lower tropospheric mean wind speed
L [km]	1000.0	40000.0	chosen to represent different length scales
$\tau = u/L$ [day^{-1}]	0.00216	0.864	computed from extreme u and L

The assumed water vapour pass distribution is characterized by one value w_{o} across the ocean atmosphere and another value w_ℓ across the land atmosphere. Hence, wind transports the moisture amount $w_{\mathrm{o}}u$ into the land domain and $w_\ell u$ into the ocean domain. Since we only have two boxes and periodic boundary conditions, the total net advection rates, $A_{\mathrm{tot,l}}$ and $A_{\mathrm{tot,o}}$, into the land and ocean domains, respectively, are identical in magnitude but with opposite signs. Translating this total advection rate into mean advection rates per unit land/ocean length gives

$$A_\ell = \frac{(w_{\mathrm{o}} - w_\ell)u}{\alpha L} \tag{9}$$

and

$$A_{\mathrm{o}} = -\frac{(w_{\mathrm{o}} - w_\ell)u}{(1-\alpha)L}, \tag{10}$$

where A_ℓ and A_{o} have units mm/day and α and L are the land fraction and full domain length, respectively, as introduced earlier.

With these parametrizations, the model has a total of 14 free parameters which we can reduce to 12 if we treat nz_{r} (in mm) as one combined parameter and introduce the characteristic rate of atmospheric transport $\tau = u/L$ in day^{-1}. Table 1 provides sensible ranges for the 12 parameters. These ranges are used to constrain the precipitation ratio across the parameter space and test the sensitivity of the model results to parameter variations.

3. Evaluation methods

In this section, we present the different analysis methods that are employed to evaluate the model behavior and assess the sensitivity of the precipitation partitioning to a variation of the model parameters. The partitioning is quantified with the precipitation ratio,

$$PR = \frac{P_\ell}{P_\mathrm{o}} = \frac{P(w_\ell)}{P(w_\mathrm{o})}. \tag{11}$$

Since we are interested in the properties of equilibrium states of the land-ocean-atmosphere system, we want to compute PR for the equilibrium values of w_ℓ and w_o. The equilibrium solution to the model equations (1) to (3) has to be found numerically. We use the `DynamicalSystems.jl` library from Datseris (2018) to find all roots of the model equations and determine whether each root represents a stable or unstable fixed point of the system.

Adopting an agnostic view on the plausibility of different combinations of parameter values from the ranges given in Table 1, we are confronted with a 12-dimensional parameter space with uniform probability distribution. A general assessment of the sensitivity of equilibrium states and related quantities to a variation of the model parameters requires a sampling of the full parameter space. To this end, we perform $n = 10000$ model simulations for randomly chosen combinations of parameter values, each yielding a corresponding fixed point.

Having obtained a sufficiently large dataset in this way, the sensitivity of a computed quantity Q to a given parameter p_i can be visually and quantitatively evaluated with Q-p_i scatter plots. The sensitivity is given by the correlation between Q and corresponding p_i values. For a potentially non-linear and non-monotonic distribution of the data points, a suitable sensitivity measure is the mutual information $MI(p_i, Q)$ which quantifies how much knowing the value of p_i will reduce the uncertainty about Q. Mutual information MI is computed as,

$$MI(p, Q) = H(p) + H(Q) - H(p, Q), \tag{12}$$

where $H(p_i)$, $H(Q)$ and $H(p_i, Q)$ are the information entropies [Shannon (1948)] of p_i and Q values and their joint distribution, respectively, where we use amplitude binning to ascribe probability distributions. We follow an approach from Datseris and Parlitz (2022) to assess the significance level for an obtained sensitivity value and to compare the sensitivity of the $i = 1, ..., 12$ different parameters. To this end, we define a mutual information index

$$I_{MI}(p_i) = \frac{MI(\hat{p}_i, Q)}{MI_{\text{uncorr},3\sigma}(\hat{p}_i, Q)}, \tag{13}$$

where $\hat{p}_i$ denotes a rescaled version of p_i with values between 0 and 1 and $MI_{\text{uncorr},3\sigma}(\hat{p}_i, Q)$ is the mutual information value that deviates by three standard deviations σ from the mean of a distribution of MI values for uncorrelated $\hat{p}_i$ and Q. A detailed description of this method is presented in Appendix [***]. $I_{MI} = 1$ is used as the significance threshold. The higher $I_{MI}(p_i)$, the more sensitive Q is to a variation of parameter p_i.

4. Closed model results

The results presented in this section are based on the data of 10000 simulations of the closed model, henceforth referred to as "CM data", which randomly sample the parameter space as explained in Section 3, each yielding the equilibrium solution for a unique point in the parameter space provided in Table 1. The section is organised in two parts. First, we discuss basic features of the system behavior, their implications for the precipitation partitioning between land and ocean, and whether constraints of the precipitation ratio exist. Second, we examine the parameter sensitivity of the precipitation ratio and which physical arguments explain these individual relationships.

a. Basic model behaviour

Figure 2 shows the probability density functions (PDF) for equilibrium soil moisture (left and middle panel) and water vapor passes for land and ocean atmospheres (right panel). In the middle panel, s is rescaled to $\tilde{s} = (s - s_{\text{pwp}})/(s_{\text{fc}} - s_{\text{pwp}})$ in order to demonstrate the relative location of the equilibrium values in the different regimes of evapotranspiration, E_ℓ, described in Section 2b. Values between the two dotted vertical lines fall into the transition regime between permanent wilting point and field capacity, in which evapotranspiration is water limited and increases strongly with s. The bulk of all simulations equilibrates at intermediate soil moisture values between $s = 0.25$ and 0.75. Due to the different choices of parameter combinations, most of these values correspond to the center part of the E_ℓ-transition regime around $\tilde{s} = 0.5$. Similarly, the atmospheres equilibrate at intermediate w_o and w_ℓ values between 40 and 50 mm, well below the saturation

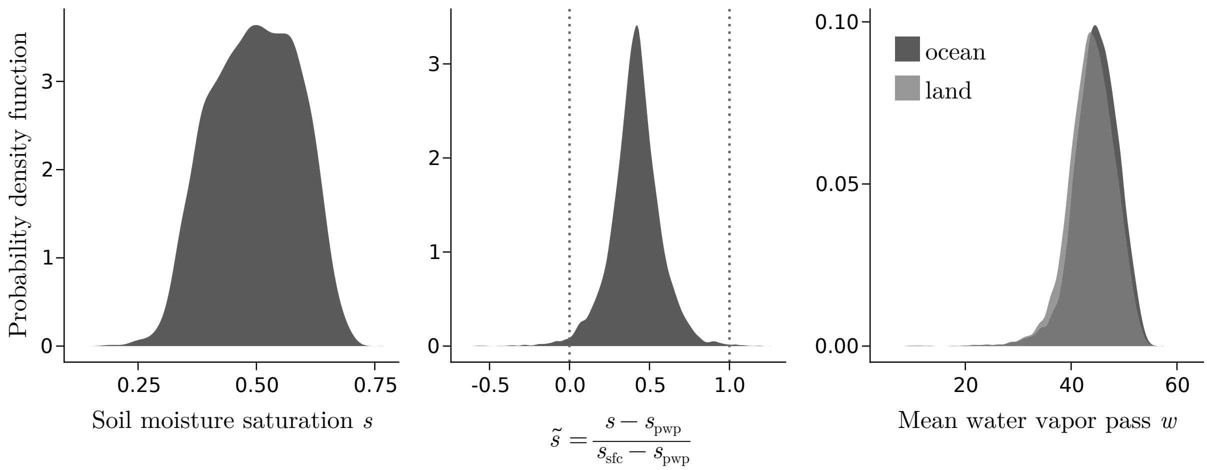

FIG. 2. Probability density functions of equilibrium soil moisture values (left panel), rescaled soil moisture values with vertical lines denoting the beginning and end of the transition regime of E_ℓ (middle panel), and mean water vapor pass of the land and ocean atmospheres (right panel).

water vapor pass values given in Tab. 1. The moisture distribution for the land atmosphere is slightly shifted towards lower values, reflecting drier conditions over land than over ocean. Only few simulations result in very dry or moist soil and atmospheric conditions. We will come back to these cases when discussing parameter sensitivities.

Figure 3 shows rolling averages of the equilibrium flux rates of land precipitation P_ℓ, ocean precipitation P_o, ocean evaporation E_o, evapotranspiration from the land surface E_ℓ, runoff R and land and ocean advection, A_ℓ and A_o, respectively, as functions of the equilibrium soil moisture saturation values s. Note that the ocean advection rate A_o has negative values for all equilibrium solutions and is therefore multiplied by -1 to simplify the comparison of its magnitude with other fluxes. Figure 3 contains the entire CM data, i.e. solutions for all different combinations of parameter values. Therefore, one should not confuse the plotted curves with well-defined functions of s with fixed parameter values. For instance, the flattening of E_ℓ (geen line) beyond $s \approx 0.35$ is unrelated to the plateau regime of the E_ℓ-parametrization of Eqn. (7) above the field capacity. We already concluded from the PDF of $\tilde{s}$ in Fig. 2 that most equilibrium soil moisture values lie in the transitional E_ℓ-regime and that the plateau regime is hardly ever attained. The shape of E_ℓ in Fig. 3 is therefore a result of averaging over equilibrium points on different realisations of Eqn. (7) corresponding to different combinations of s_pwp, s_fc and E_p values.

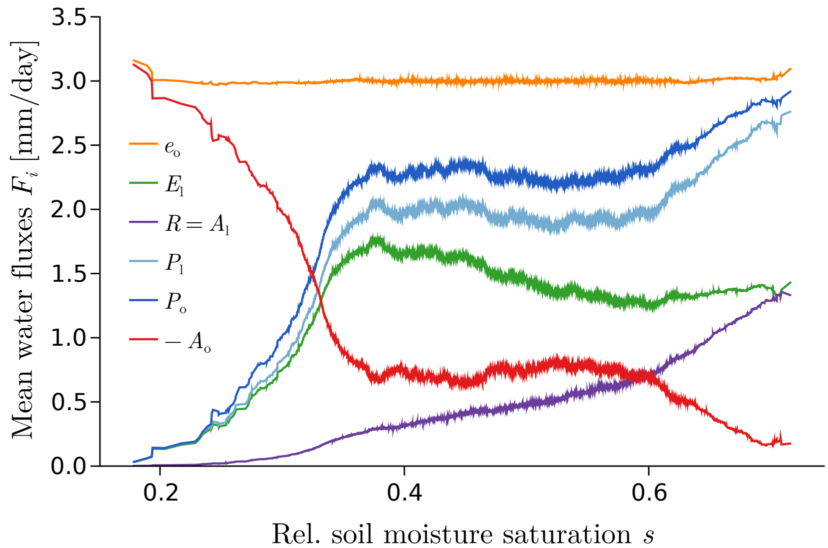

FIG. 3. Symmetric rolling average of equilibrium fluxes versus soil moisture saturation computed from CM data. For evapotranspiration (green line), the individual data points are shown as scatter plots and the range of $E_\ell(s)$ parametrizations for different parameter combinations is shaded in light green.

Even though we cannot readily understand the diverse interplay of different parameter choices from Figure 3, three qualitative observations allow for drawing first conclusions about the partitioning of precipitation in the land-ocean-atmosphere system:

1. Land advection, A_ℓ (purple line) is strictly positive, meaning that moisture is always supplied by the ocean atmosphere to the land atmosphere. This net advection to the land compensates for the soil's constant loss of water through runoff, i.e. $A_\ell = R$. This compensation mechanisms in equilibrated hydrological systems has already been established in earlier studies by Horton (1943) or Peixóto and Oort (1983).

2. According to Equations (9) and (10), the net water transport from ocean to land requires the ocean atmosphere to be moister than the land atmosphere, $w_o > w_\ell$. Since the same, monotonically increasing function $P(w)$ from Eqn. (6) is used for both land and ocean precipitation, this implies that P_o is larger than P_ℓ. In other words, mean precipitation is always stronger over ocean than over land. This is confirmed by Fig. 3 where the dark blue curve for P_o always lies above the bright blue curve for P_ℓ. As a direct consequence, the precipitation ratio is bound by an upper limit of one, i.e. $PR < 1$.

3. All fluxes lie within the open interval $(0, e_o)$, i.e. no other mean flux can become larger than the ocean evaporation rate (orange line). This can be explained as follows: e_o is partitioned into ocean precipitation P_o and ocean advection $|A_o|$ so that each of the two components needs to be smaller than e_o. Since the land atmosphere is drier than the ocean atmosphere, it follows that $P_\ell < P_o < e_o$. Land precipitation can be written as the sum of fluxes, $P_\ell = E_\ell + R = E_\ell + A_\ell$, so that again, each of these components needs to be smaller than e_o.

The shapes of the lines in Figure 3 indicate that three soil moisture regimes can be distinguished: For low soil moistures up to $s \approx XXX$, runoff and advection are negligible and precipitation follows the shape of E_ℓ. In an intermediate soil moisture regime, $XXX \lesssim s \lesssim XXX$, precipitation flattens due to a balancing effect of decreasing evapotranspiration and increasing advection. Lastly, above $s \approx XXX$, E_ℓ remains nearly constant. Increasing advection dominates this regime and leads to a rise in precipitation. Here, I could cite Salvucci and/or Lintner but I am not sure to which extent their results are comparable to mine and whether it is wise to make a comparison.. Understanding these regimes requires a deeper understanding of parameter sensitivities and how different parameters interact. For instance, we will see that low s values are only attained when the land fraction is sufficiently large and that high s values require a high permanent wilting point as well as efficient atmospheric transport. Such considerations will also resolve the apparent contradiction of an overall declining moisture advection out of the ocean atmosphere (red line) while the advection into the land atmosphere (purple line) is monotonically increasing over the range of s.

Note: Everything below has not yet been reworked. So you don't need to read any further :) My plan however is to continue with briefly describing the shape of the fluxes in Fig. 2, pointing out that there seem to be three regimes: For low s, precipitation (blue lines) follows land evapotranspiration (green line) fairly closely while runoff/advection (purple line) is negligible. For intermediate s, precipitation rests in a plateau phase in which decreasing E_ℓ is balanced by increasing runoff/advection. For highest s, precipitation is eventually dominated by runoff/advection. This behaviour cannot be understood by looking at the parametrisations or model equations alone. Rather, the influence of different parameters is encoded in it (e.g. low s values correspond to high α, highest s values share a high permanent wilting point etc.). This will be my link to the next section of the results, i.e. parameter sensitivities. I don't know if this will work out but ideally, I would like to briefly return to Fig. 2 after having discussed the dominant parameter sensitivities and piece things together, so that the reader understands why the fluxes in Fig. 2 look the way they do.

The behaviour of the fluxes for different soil moisture values in Figure 3 can be roughly divided into three regimes. The first regime extends from the lowest soil moisture values up to about $s \approx 0.35$ and is characterized by a sharp

b. Parameter sensitivity of PR

Building on the preceding general description of the model behavior, we now draw our attention to the sensitivity of the precipitation ratio with respect to a variation of different model parameters. Three parameters stand out in having a particularly strong impact on PR: Land fraction α, atmospheric moisture transport parameter τ and permanent wilting point s_{pwp}. We discuss the underlying relationships using the same CM data as before.

Land fraction α: Figure 5 shows a scatter plot of PR values over α. Despite considerable spread in PR, we can see that $PR \to 1$ for both limits, $\alpha \to 0$ and $\alpha \to 1$. This reflects very similar moisture conditions in the two atmospheres when α is extreme. Knowing that $w_{\text{o}} > w_\ell$ for all equilibrium states, it follows that PR will only decrease if $\Delta w = w_{\text{o}} - w_\ell$ increases. As has been discussed in the preceding section, the system's equilibrium states for a tiny land domain are relatively moist. For $\alpha \to 0$, a large Δw cannot be sustained since the resulting advection amount $\Delta w u$ would translate to a large land advection rate, $\Delta w u/(\alpha L)$, that would immediately moisten the land atmosphere and assimilate w_{o} and w_ℓ. On the other end of the range, when the ocean is tiny, i.e. $\alpha \to 1$, large moisture differences are likewise impossible: This time, Δw is limited by the total amount of water that enters the system through the ocean surface. The ocean atmosphere cannot export more water than it receives. Therefore, the total amount of evaporated water sets the upper limit for advection, $\Delta w\, u < (1-\alpha) L\, e_{\text{o}}$. This amount decreases with increasing α, so that Δw needs to decrease with it. Moreover, Δw needs to stay below this limit since the ocean atmosphere has to stay moister than the land atmosphere to facilitate advection in the first place.

Along the mid-α range, PR decreases until it reaches a minimum beyond which the ratio increases again. This behaviour is somewhat concealed by the large spread in PR for intermediate land fractions but is both visible in the means of bins of 100 consecutive α values (dark grey line) and in graphs for which all parameters except α were kept fixed (not shown). A mathematically

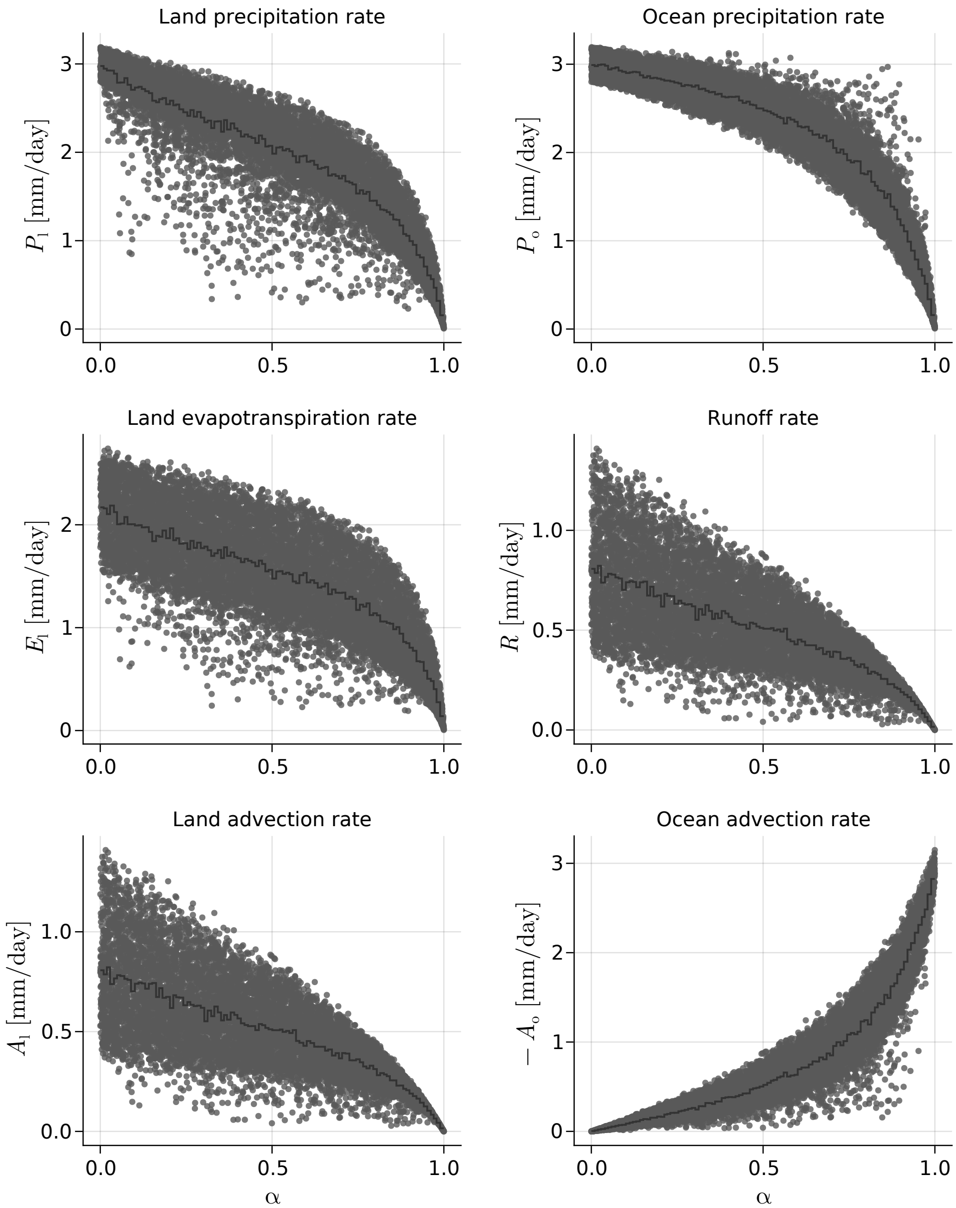

FIG. 4. Mean water fluxes computed from the equilibrium states of 10000 closed model runs with randomly sampled parameter values and plotted over land fraction α. The dark grey line shows the mean values of bins of 100 consecutive α-values. The negative ocean advection rate A_o reflects a net transport of water out of the ocean and into the land atmosphere. Multiplication by -1 simplifies the comparison of its magnitude with the other flux quantities.

rigorous analysis of $PR(\alpha)$ in this range and, in particular, the location of the minimum is difficult due to the lack of an analytical expression for the relationship between precipitation ratio and land fraction. We can write,

$$PR(\alpha) = \frac{P_\ell(\alpha)}{P_o(\alpha)} = \frac{E_\ell(s) + \frac{(w_o - w_\ell)u}{\alpha L}}{e_o - \frac{(w_o - w_\ell)u}{(1-\alpha)L}}, \tag{14}$$

but we may not overlook the fact that our state variables are implicit functions of α, too, i.e. $s(\alpha)$, $w_o(\alpha)$ and $w_\ell(\alpha)$. Even though we don't know the analytical form of these state variable dependencies, Eqn. (5) gives a useful indication of why the precipitation ratio should decrease for small but increasing α and why it should increase again as α approaches one. This indication lies in the factors $f = 1/\alpha$ and $g = 1/(1-\alpha)$ in the land and ocean advection rates, respectively. Assuming that the system resides in an equilibrium state for some α close to zero, a small increase in α would lead to a rather strong drop in the land advection rate (strong negative slope of f at low α) compared to the rather mild increase in the magnitude of ocean advection (weakly positive slope of g at low α)...

I stopped here because I wondered if it makes sense to explain the shape of $PR(\alpha)$ in such great detail. Maybe all this could be described in a much simpler way by starting from total moisture input rather than mean rates. The argument would go something like this: increasing land = generally less water available to the circulation in the system. Consequently, the moisture state as a whole must become drier, i.e. all state variables decrease but at different rates. Land precip (and with it w_ℓ) decrease both trough a reduction of E_ℓ and a rather sharp drop in A_ℓ due to factor f. Ocean precip only decreases by slight increase of $-A_o$. For large α the system is already in a rather dry state. E_ℓ decreases only slightly with decreasing s and impact of f is less strong. For ocean precip, the opposite is true. Here, g plays a stronger role now and increases the ocean advection rate strongly. In the end, the interplay of the different nonlinear parametrisations make the behaviour of PR asymmetric around $\alpha = 0.5$ and hard to understand in detail.

Atmospheric rate of transport τ: The ratio between mean horizontal wind speed and spatial extent of the model, $\tau = u/L$, is a measure for the efficiency with which moisture is transported across the model atmosphere. Its inverse value, τ^{-1}, corresponds to the time that an air parcel would need to travel across the full domain length L. In the advection terms of Eqn. (2) and (3), τ appears as the rate at which moisture is moved across the boundaries between the two atmospheric

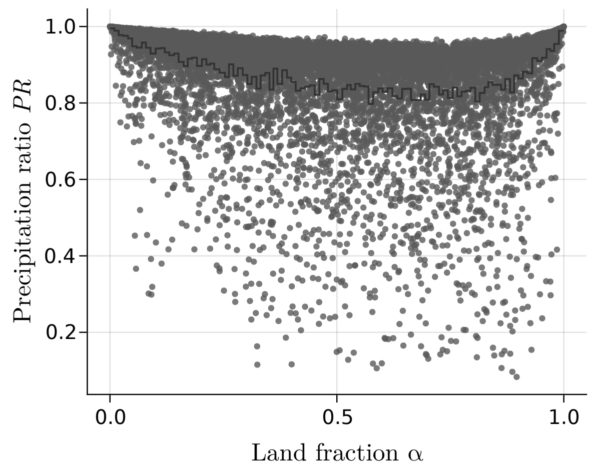

FIG. 5. Smile plot

boxes. It has therefore major implications for the ability of advection to assimilate the moisture conditions over ocean and land. A very small value of τ, i.e. a low rate of transport, corresponds to a combination of large domain size and low wind speed while a small domain and strong wind result in a very large value of τ. Assuming a fixed land fraction α, a larger moisture difference Δw is needed to move the same total amount of water across a box boundaries when the rate of transport is small, compared to when it is large. Except for the special cases of extreme land fractions, $\alpha \rightarrow \{0, 1\}$, where α enforces very similar moisture conditions over land and ocean, it is primarily τ that sets the moisture difference which is needed to attain the equilibrium state. This dominant role is illustrated in Figure 6 which shows the scatter plot of precipitation ratio over τ. While we already assessed that α sets the overall upper limit of PR, Fig. 6 shows that τ sets the overall lower bound. It explains the large spread for PR values in the mid-α range in Figure 5, where the efficiency of atmospheric moisture transport is particularly important. Only high rates of transport enable the system to attain an equilibrium state with rather similar moisture conditions over land and ocean. For instance, if $\tau > 0.4\,\mathrm{day}^{-1}$, then PR stays above 0.8 regardless of the choice of values for other parameters. Note, that τ combines the information about both wind and spatial extent of the model. If one fixes one of the two, e.g. $L = 40000\,\mathrm{km}$ to simulate the full Tropics along the equator, the physically sensible range of τ is limited. For example, in order to obtain a rate of transport larger than $0.4\,\mathrm{day}^{-1}$, such a large L would require a minimum wind speed of 185 m/s, a value that lies beyond the highest wind speed ever measured on Earth. More realistic

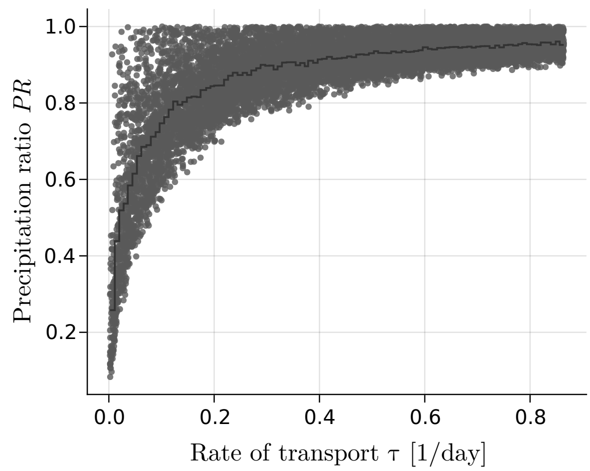

FIG. 6. τ-dependence

mean wind speed values for such a large domain could lie around 5 to 10 m/s with corresponding rates of transport, $\tau \approx 0.01 - 0.02$. At these low values of τ, the spread of PR values is considerable which means that also other parameters have a substantial influence on the attained equilibrium state.

Permanent wilting point $s_{\mathbf{pwp}}$: It takes work to extract water from the soil and the drier the soil, the more work is needed to facilitate evapotranspiration. Regardsless of whether the land surface is bare or covered with vegetation, s_{pwp} is a characteristic property of the soil type which denotes the relative soil moisture saturation value below which practically no water can be extracted. The left panel of Figure 7 shows the parametrization function of evapotranspiration, $E_\ell(s)$, for different choices of the permanent wilting point. For instance, $s_{\text{pwp}} \approx 0.3$ might correspond to loam and $s_{\text{pwp}} \approx 0.5$ to clay (Hagemann and Stacke (2015)). In the evapotranspiration graphs, s_{pwp} determines the soil moisture value at which the curve transitions from $E_\ell \approx 0$ to the regime of steeply increasing E_ℓ. Since the field capacity s_{fc} lies $\Delta s = 0.3$ higher than s_{pwp} for all relevant soil types, a change in s_{pwp} merely shifts the evapotranspiration graph along the s-direction, while its shape remains unchanged.

Figure 8 shows a negative trend of the precipitation ratio with increasing s_{pwp} for the performed model runs. The impact of soil type on the precipitation ratio is weaker than, for example, the impact of τ but it is nonetheless clearly visible and s_{pwp} represents the third most sensitive model parameter. To understand the dependence of PR on s_{pwp}, it is convenient to think of a system in equilibrium for some permanent wilting point, e.g. $s_{\text{pwp}} = 0.3$. The mean equilibrium soil moisture value in the CM data for $s_{\text{pwp}} = 0.3$ is $s = 0.43$. This initial state of the model is displayed as a blue dot in Figure 7. An abrupt increase of s_{pwp} to $s_{\text{pwp}} = 0.4$ leads to a significant drop of E_ℓ as illustrated by the first red arrow connecting the blue and green dot in the left panel of Fig. 7. The green dot represents a temporary state where the model is not in equilibrium because the state variables have not yet adapted to the new situation. At this point, the soil receives the same amount of precipitation but loses less water through evapotranspiration. As a result, the soil moistens. As time progresses, the system attains a new equilibrium state at a higher s value which is marked by the orange dot. This moistening of the soil is shown in the right panel of Fig. 7, where the equilibrium s values of the CM data are plotted over the corresponding values of s_{pwp}. However, as s increases, runoff and land advection rate increase, too. Assuming that $\tau/(\alpha L)$ is kept fixed, Δw has to increase to facilitate the increase of advection. The water that is supplied to the land atmosphere as advection is taken from the ocean atmosphere, where w_{o} decreases as a consequence. Hence, an increase in advection is only possible, if w_ℓ decreases more strongly than w_{o}. The increase in R combined with a decrease in P_ℓ is the reason why the new equilibrium state for $s_{\text{pwp}} = 0.4$ will have a moister soil but a lower evapotranspiration rate than the initial state for $s_{\text{pwp}} = 0.3$. The fact that w_ℓ must decrease more strongly than w_{o} in the adaptation process is the reason why PR declines with increasing s_{pwp}.

5. Open model formulation

The closed model discussed so far can be applied to any system for which the total net advection is zero. Such conditions might be met in the real world when we look at very large scales, e.g. global domains such as the tropical band. However, in the case of more local, small scale phenomena, the net advection might not be zero and the situation is better captured by an open model configuration, where moisture inflow at the windward model boundary is a model parameter and no constraints apply to the moisture outflow at the leeward boundary. In this model configuration, the modelled domain can have a net advection larger or smaller than zero. In the following, we present the formalism and analysis of an open model with two oceanic domains and an island inbetween them.

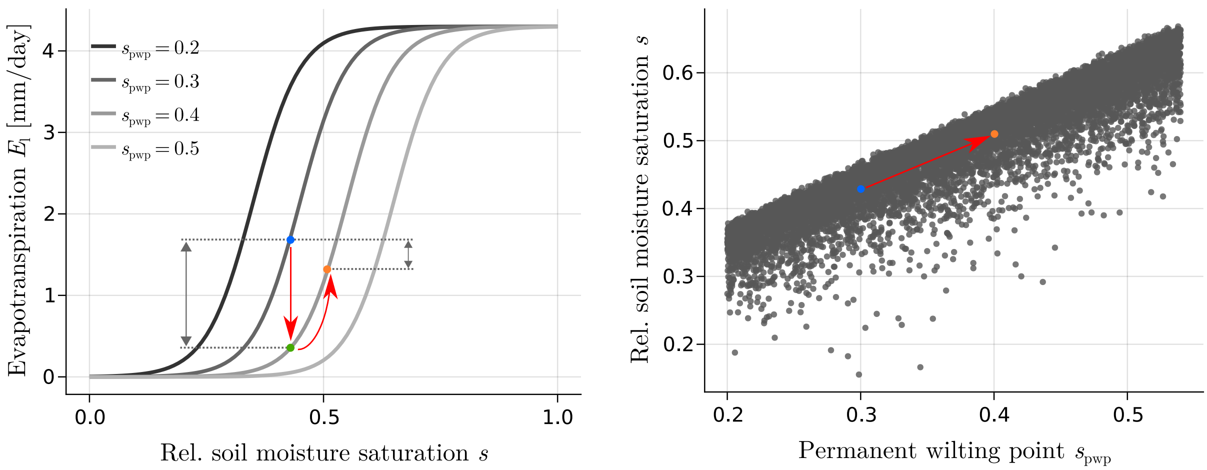

FIG. 7. Influence of an increase in s_{pwp} on the equilibrium state. Left: Higher values of s_{pwp} shift the graph of the E_ℓ parametrization towards larger s. Right: Equilibrium values of the soil moisture saturation from CM data plotted over s_{pwp} values. In left panel, next to left black arrows will stand something like ΔE_{inst} for instantaneous E_ℓ-difference and next to the right black arrows ΔE_{eq} to denote the E_ℓ difference between old and new equilibrium state.

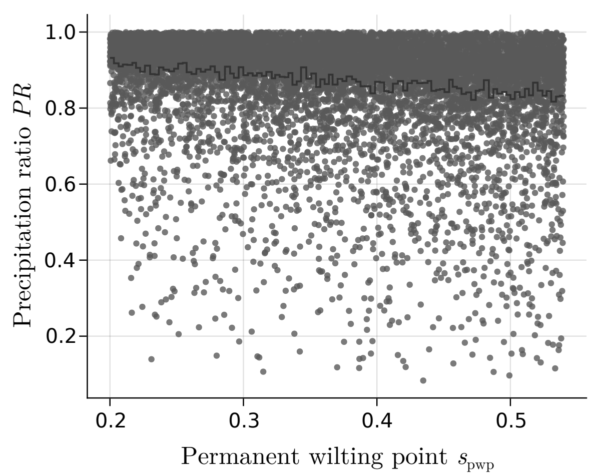

FIG. 8. s_{pwp}-dependence

a. Open model equations

The model equations for an open configuration are similar to the ones for the closed model. This time, four instead of three equations are needed as the system has now one more ocean domain. The meaning of the soil moisture variable s is unchanged, while a different notation is employed for the water content of the atmospheric boxes. The index $i = 1, 2, 3$ is used to denote the mean integrated water vapour pass w_i and net advection rate A_i of the first ocean atmosphere ($i = 1$), land atmosphere ($i = 2$) and second ocean atmosphere ($i = 3$), respectively. With this, the model equations read

$$\frac{ds}{dt} = \frac{1}{nz_\mathrm{r}}\left[P(w_2) - R(s, w_2) - E(s)\right] \tag{15}$$

$$\frac{dw_1}{dt} = e_\mathrm{o} - P(w_1) + A_1 \tag{16}$$

$$\frac{dw_2}{dt} = E(s) - P(w_2) + A_2 \tag{17}$$

$$\frac{dw_3}{dt} = e_\mathrm{o} - P(w_3) + A_3, \tag{18}$$

with

$$A_\mathrm{i} = \frac{(w_{\mathrm{i}-1} - w_\mathrm{i})u}{L_\mathrm{i}}. \tag{19}$$

Note, that a new parameter w_0 was introduced which denotes the boundary condition of the water vapor pass at the windward end of the model domain. It reflects the synoptic scale? conditions which the model is embedded in.

b. Open model results

- How the open model relaxes the condition that PR<1 (PR>1 only under certain rare conditions)
- The role of synoptic moisture conditions in the atmosphere
- Open model can be transformed into the closed model

6. Discussion

- Which aspects of this study change the way we look at precipitation partitioning? (Especially, which relationships were not clear from the start?)
- Which conditions need to be met to end up with a precipitation ratio larger one, what role does a correct parametrization of precipitation play in this respect?

- What are possible use cases for the models?
- What can the model(s) tell us and what not and why? (e.g. land distribution not representative for the Tropics)
- We make ET purely dependent on soil moisture which ignores the fact that atmospheric conditions feed back on the ET rate. This coupling of land and atmosphere might be important and is not represented in our model. Schaefli et al. say that a decoupling of this kind leads to an overestimation of soil filling (too high s).

7. Conclusions

This study was motivated by our lack of theoretical understanding of how Earth's total precipitation gets partitioned between land and ocean. More precisely, we wanted to know which physical processes and quantities determine the partitioning and whether the range of plausible values for these quantities sets constraints on the ratio between spatio-temporal mean land and ocean precipitation, $PR = P_\ell / P_\mathrm{o}$.

To this end, we introduce a conceptual water balance model that describes the rate of change of soil moisture and atmospheric moisture over ocean and land, respectively. Drawing inspiration from earlier works by Rodriguez-Iturbe et al. (1991) and Bretherton et al. (2004), the water balance components are expressed as functions of the mean water content of the land and atmospheric subdomains. These functions contain several environmental parameters, some of which can be assumed to stay constant on human timescales, e.g. Earth's land fraction, and others that might change in a changing climate such as mean horizontal wind speed or properties of the soil. Assuming that the Earth system's moisture state is a steady state on the timescale of a couple of years, we analyze a large number of equilibrium solutions for different combinations of model parameter values. The obtained results can be summarized as follows:

- To reach equilibrium, the fundamental property of soil to lose water through runoff demands a net atmospheric moisture transport from the ocean to the land and a runoff return flow of identical magnitude from soil to ocean. In a closed, two-domain model, the ocean atmosphere will therefore equilibrate at a moister value than the land atmosphere. If the same relationship between precipitation and atmospheric moisture holds for land and ocean regions, then the precipitation ratio is bound by an upper limit of $PR = 1$.

- The lower bound of the precipitation ratio is mostly determined by the atmospheric moisture transport parameter, $\tau = u/L$. Efficient advection (large τ) results in similar moisture conditions over land and ocean and, hence, similar precipitation rates, while inefficient advection (low τ) leads to large moisture differences and an ocean precipitation up to ten times as strong as over land ($PR \approx 0.1$). Significant sensitivity is also found to a variation of land fraction α and to a lesser extent to the permanent wilting point and field capacity of the soil. The land fraction is most relevant near its extreme values of a large ocean and small land, $\alpha \rightarrow 0$, where the overall moisture state of the model is wet and of a small ocean and large land where the moisture state is dry. In both extreme cases, the precipitation ratio attains values close to one. In contrast, for intermediate values, the land fraction loses much of its predictive power and the influence of τ dominates.

- The conceptual water balance model has difficulties explaining observed island precipitation enhancement. Although precipitation ratios larger than one are found for an open model configuration which is more apt for simulating the spatial scales of islands, these cases of precipitation enhancement make up for only a rather small subset of the parameter space which is characterized by small land sizes, rather large water vapor pass boundary values and a tendency for small values of τ. A necessary condition for land precipitation enhancement in this model framework is a moisture cascade along the wind trajectory.

Although these findings suggest a rather strong and qualitatively robust sensitivity of precipitation partitioning to certain physical properties of the Earth system, we have to keep in mind that the employed model equations are the product of a number of strong assumptions. Foremost, we assumed the same precipitation parametrization to hold over land and ocean. It is likely that this is not justified. Knowing whether the same mean water vapour pass will result in more or less precipitation over land compared to over ocean would clarify whether the precipitation ratio can become larger than one on global scales. An appropriate observational investigation of this relationship is therefore a possible direction for future studies. Another limitation of this study that might have a qualitative influence on the inferred bounds of the precipitation ratio is the role of land distributions. Configurations with more than one land box require additional model equations and will exhibit different equilibrium states for the same choice of model parameter values compared to the two-domain model configuration.

Lastly, the pure water balance approach explored in this study is insufficient to cover the full range of physical processes that are evoked by land-ocean differences. Especially the different ways in which the two surfaces partition incoming energy into sensible and latent heat fluxes might have a major indirect impacts on the partitioning of precipitation. For instance, it is plausible that sea breezes could temporarily transport more moisture into the land atmosphere, causing high rain rates due to the nonlinear dependence of precipitation on water vapor pass. In such a scenario, the ocean atmosphere could still be moister than the land atmosphere on average but mean precipitation over land might be higher even when using the same parametrization $P(w)$. Particularly in the context of island precipitation enhancement, energy considerations might be indispensable. Extending the model framework by energy balance equations or incorporating the effect of the diurnal cycle indirectly through energy-dependent parameters promises to yield a more complete theoretical understanding of precipitation partitioning.

Acknowledgments.

Data availability statement.

References

Bretherton, C. S., M. E. Peters, and L. E. Back, 2004: Relationships between water vapor path and precipitation over the tropical oceans. *J. Climate*, **17**, 1517–1528, https://doi.org/10.1175/1520-0442(2004)017<1517:RBWVPA>2.0.CO;2.

Brubaker, K., D. Entekhabi, and P. Eagleson, 1991: Atmospheric water vapor transport: Estimation of continental precipitation recycling and parameterization of a simple climate model. URL https://ntrs.nasa.gov/citations/19910018381.

Brubaker, K. L., D. Entekhabi, and P. S. Eagleson, 1993: Estimation of continental precipitation recycling. *Journal of Climate*, **6**, 1077–1089, https://doi.org/10.1175/1520-0442(1993)006<1077:EOCPR>2.0.CO;2, URL https://journals.ametsoc.org/jcli/article/6/6/1077/39303/Estimation-of-Continental-Precipitation-Recycling.

Budyko, M. I., 1956: *Heat balance of the Earth's surface*. U.S. Dept. of Commerce, Weather Bureau.

Budyko, M. I., and O. A. Drozdov, 1953: Characteristics of the moisture circulation in the atmosphere. **4**, 5–14.

Burde, G. I., and A. Zangvil, 2001: The estimation of regional precipitation recycling. part i: Review of recycling models. *Journal of Climate*, **14 (12)**, 2497–2508, https://doi.org/10.1175/1520-0442(2001)014<2497:TEORPR>2.0.CO;2, URL https://journals.ametsoc.org/jcli/article/14/12/2497/29526/The-Estimation-of-Regional-Precipitation-Recycling.

Cronin, T. W., K. A. Emanuel, and P. Molnar, 2015: Island precipitation enhancement and the diurnal cycle in radiative-convective equilibrium. **141 (689)**, 1017–1034, https://doi.org/10.1002/qj.2443, URL https://rmets.onlinelibrary.wiley.com/doi/abs/10.1002/qj.2443.

Datseris, G., 2018: Dynamicalsystems.jl: A julia software library for chaos and nonlinear dynamics. *Journal of Open Source Software*, **3**, 598, https://doi.org/10.21105/joss.00598.

Datseris, G., and U. Parlitz, 2022: *Nonlinear Dynamics*. 2192-4791, Springer International Publishing, URL https://link.springer.com/book/9783030910334.

Eltahir, E. a. B., and R. L. Bras, 1994: Precipitation recycling in the amazon basin. *Quarterly Journal of the Royal Meteorological Society*, **120**, 861–880, https://doi.org/10.1002/qj.49712051806, URL https://onlinelibrary.wiley.com/doi/abs/10.1002/qj.49712051806.

Ent, R. J. v. d., H. H. G. Savenije, B. Schaefli, and S. C. Steele-Dunne, 2010: Origin and fate of atmospheric moisture over continents. *Water Resources Research*, **46 (9)**, https://doi.org/10.1029/2010WR009127, URL https://agupubs.onlinelibrary.wiley.com/doi/abs/10.1029/2010WR009127.

Entekhabi, D., I. Rodriguez-Iturbe, and R. L. Bras, 1992: Variability in large-scale water balance with land surface-atmosphere interaction. *Journal of Climate*, **5**, 798–813, https://doi.org/10.1175/1520-0442(1992)005<0798:VILSWB>2.0.CO;2, URL https://journals.ametsoc.org/jcli/article/5/8/798/35919/Variability-in-Large-Scale-Water-Balance-with-Land.

Fiedler, S., and Coauthors, 2020: Simulated tropical precipitation assessed across three major phases of the coupled model intercomparison project (CMIP). *Monthly Weather Review*, **148 (9)**, 3653–3680, https://doi.org/10.1175/MWR-D-19-0404.1.

Findell, K. L., and E. A. B. Eltahir, 2003: Atmospheric controls on soil moisture–boundary layer interactions. part i: Framework development. *Journal of Hydrometeorology*, **4 (3)**, 552–569, https://doi.org/10.1175/1525-7541(2003)004<0552:ACOSML>2.0.CO;2, URL https://journals.ametsoc.org/jhm/article/4/3/552/68951/Atmospheric-Controls-on-Soil-Moisture-Boundary.

Froidevaux, P., L. Schlemmer, J. Schmidli, W. Langhans, and C. Schär, 2014: Influence of the background wind on the local soil moisture–precipitation feedback. *Journal of the Atmospheric Sciences*, **71 (2)**, 782–799, https://doi.org/10.1175/JAS-D-13-0180.1, URL https://journals.ametsoc.org/doi/10.1175/JAS-D-13-0180.1.

Hagemann, S., and T. Stacke, 2015: Impact of the soil hydrology scheme on simulated soil moisture memory. *Climate Dyn.*, **44**, 1731–1750, https://doi.org/10.1007/s00382-014-2221-6.

Hohenegger, C., P. Brockhaus, C. S. Bretherton, and C. Schär, 2009: The soil moisture–precipitation feedback in simulations with explicit and parameterized convection. *Journal of Climate*, **22 (19)**, 5003–5020, https://doi.org/10.1175/2009JCLI2604.1, URL https://journals.ametsoc.org/jcli/article/22/19/5003/32298/The-Soil-Moisture-Precipitation-Feedback-in.

Hohenegger, C., and B. Stevens, 2018: The role of the permanent wilting point in controlling the spatial distribution of precipitation. *Proceedings of the National Academy of Sciences*, **115 (22)**, 5692–5697, https://doi.org/10.1073/pnas.1718842115, URL https://www.pnas.org/content/115/22/5692.

Horton, R. e., 1943: Hydrologic interrelations between lands and oceans. *Eos, Transactions American Geophysical Union*, **24 (2)**, 753–764, https://doi.org/10.1029/TR024i002p00753, URL https://onlinelibrary.wiley.com/doi/abs/10.1029/TR024i002p00753.

Lynn, B. H., W.-K. Tao, and P. J. Wetzel, 1998: A study of landscape-generated deep moist convection. *Monthly Weather Review*, **126 (4)**, 928–942, https://doi.org/10.1175/1520-0493(1998)126<0928:ASOLGD>2.0.CO;2, URL https://journals.ametsoc.org/mwr/article/126/4/928/66256/A-Study-of-Landscape-Generated-Deep-Moist.

Manabe, S., 1969: CLIMATE AND THE OCEAN CIRCULATION: I. THE ATMOSPHERIC CIRCULATION AND THE HYDROLOGY OF THE EARTH's SURFACE. *Monthly Weather Review*, **97 (11)**, 739–774, https://doi.org/10.1175/1520-0493(1969)097<0739:CATOC>2.3.CO;2, URL https://journals.ametsoc.org/view/journals/mwre/97/11/1520-0493_1969_097_0739_catoc_2_3_co_2.xml.

Peixóto, J. P., and A. H. Oort, 1983: The atmospheric branch of the hydrological cycle and climate. *Variations in the Global Water Budget*, Springer Netherlands, 5–65, https://doi.org/10.1007/978-94-009-6954-4_2, URL https://doi.org/10.1007/978-94-009-6954-4_2.

Qian, J.-H., 2008: Why precipitation is mostly concentrated over islands in the maritime continent. *Journal of the Atmospheric Sciences*, **65 (4)**, 1428–1441, https://doi.org/10.1175/2007JAS2422.1, URL https://journals.ametsoc.org/jas/article/65/4/1428/26793/Why-Precipitation-Is-Mostly-Concentrated-over.

Rodriguez-Iturbe, I., D. Entekhabi, and R. L. Bras, 1991: Nonlinear dynamics of soil moisture at climate scales: 1. stochastic analysis. *Water Resources Research*, **27**, 1899–1906, https://doi.org/10.1029/91WR01035.

Schär, C., D. Lüthi, U. Beyerle, and E. Heise, 1999: The soil–precipitation feedback: A process study with a regional climate model. *Journal of Climate*, **12 (3)**, 722–741, https://doi.org/10.1175/1520-0442(1999)012<0722:TSPFAP>2.0.CO;2, URL https://journals.ametsoc.org/jcli/article/12/3/722/28833/The-Soil-Precipitation-Feedback-A-Process-Study.

Segal, M., and R. W. Arritt, 1992: Nonclassical mesoscale circulations caused by surface sensible heat-flux gradients. *Bulletin of the American Meteorological Society*, **73 (10)**, 1593–1604, https://doi.org/10.1175/1520-0477(1992)073<1593:NMCCBS>2.0.CO;2, URL https://journals.ametsoc.org/view/journals/bams/73/10/1520-0477_1992_073_1593_nmccbs_2_0_co_2.xml.

Seneviratne, S. I., T. Corti, E. L. Davin, M. Hirschi, E. B. Jaeger, I. Lehner, B. Orlowsky, and A. J. Teuling, 2010: Investigating soil moisture–climate interactions in a changing climate: A review. **99 (3)**, 125–161, https://doi.org/10.1016/j.earscirev.2010.02.004, URL https://www.sciencedirect.com/science/article/pii/S0012825210000139.

Shannon, C. E., 1948: A mathematical theory of communication. *The Bell System Technical Journal*, **27 (3)**, 379–423, https://doi.org/10.1002/j.1538-7305.1948.tb01338.x.

Sobel, A. H., C. D. Burleyson, and S. E. Yuter, 2011: Rain on small tropical islands. *Journal of Geophysical Research: Atmospheres*, **116**, https://doi.org/10.1029/2010JD014695, URL https://agupubs.onlinelibrary.wiley.com/doi/abs/10.1029/2010JD014695.

Ulrich, M., and G. Bellon, 2019: Superenhancement of precipitation at the center of tropical islands. *Geophysical Research Letters*, **46 (24)**, 14 872–14 880, https://doi.org/10.1029/2019GL084947, URL https://agupubs.onlinelibrary.wiley.com/doi/abs/10.1029/2019GL084947.

Wang, S., and A. H. Sobel, 2017: Factors controlling rain on small tropical islands: Diurnal cycle, large-scale wind speed, and topography. *Journal of the Atmospheric Sciences*, **74 (11)**, 3515–3532, https://doi.org/10.1175/JAS-D-16-0344.1, URL https://journals.ametsoc.org/jas/article/74/11/3515/42168/Factors-Controlling-Rain-on-Small-Tropical-Islands.

Zangvil, A., D. H. Portis, and P. J. Lamb, 1993: Diurnal variations in the water vapor budget components over the midwestern united states in summer 1979. *Interactions Between Global Climate Subsystems*, American Geophysical Union (AGU), 53–63, https://doi.org/10.1029/GM075p0053, URL https://onlinelibrary.wiley.com/doi/abs/10.1029/GM075p0053.